Depletion-Mediated Red Blood Cell Aggregation in Polymer Solutions

Björn Neu and Herbert J. Meiselman
Department of Physiology and Biophysics, Keck School of Medicine, University of Southern California, Los Angeles, California 90033, USA

ABSTRACT Polymer-induced red blood cell (RBC) aggregation is of current basic science and clinical interest, and a depletion-mediated model for this phenomenon has been suggested; to date, however, analytical approaches to this model are lacking. An approach is thus described for calculating the interaction energy between RBC in polymer solutions. The model combines electrostatic repulsion due to RBC surface charge with osmotic attractive forces due to polymer depletion near the RBC surface. The effects of polymer concentration and polymer physicochemical properties on depletion layer thickness and on polymer penetration into the RBC glycocalyx are considered for 40 to 500 kDa dextran and for 18 to 35 kDa poly (ethylene glycol). The calculated results are in excellent agreement with literature data for cell-cell affinities and with RBC aggregation-polymer concentration relations. These findings thus lend strong support to depletion interactions as the basis for polymer-induced RBC aggregation and suggest the usefulness of this approach for exploring interactions between macromolecules and the RBC glycocalyx.

INTRODUCTION

The reversible aggregation of human red blood cells (RBC) continues to be of interest in the field of hemorheology (Chien et al., 1977; Cloutier and Qin, 1997; Evans and Buxbaum, 1981; Evans and Parsegian, 1983; Holley et al., 1999; Hovav et al., 1999; Kounov and Petrov, 1999; Lim et al., 1997; Lowe, 1988; Meiselman et al., 1999; Sennaoui et al., 1997; Stoltz et al., 1999) in that RBC aggregation is a major determinant of the in vitro rheological properties of blood. In addition, the in vivo flow dynamics and flow resistance of blood are influenced by RBC aggregation (Cabel et al., 1997). There is now general agreement regarding the correlations between elevated levels of fibrinogen or other large plasma proteins and enhanced RBC aggregation, and the effects of molecular mass and concentration on RBC aggregation for neutral polymers such as dextran (Chien and Lang, 1987). However, the specific mechanisms involved in RBC aggregation have not yet been elucidated.

At present, there are two co-existing "models" for RBC aggregation: bridging and depletion. In the bridging model, red cell aggregation is proposed to occur when the bridging forces due to the adsorption of macromolecules onto adjacent cell surfaces exceed disaggregation forces due to electrostatic repulsion, membrane strain, and mechanical shearing (Brooks, 1973, 1988; Chien, 1975; Chien and Jan, 1973; Chien and Lang, 1987). The depletion model proposes that RBC cell aggregation occurs as a result of a lower localized protein or polymer concentration near the cell surface as compared with the suspending medium (i.e., relative depletion near the cell surface). This exclusion of macromolecules near the cell surface leads to an osmotic gradient and thus depletion interaction (Bäumler et al., 1996). As with the bridging model, disaggregation forces are electrostatic repulsion, membrane strain, and mechanical shearing.

Several previous reports have dealt with the experimental and theoretical aspects of depletion aggregation, often termed depletion flocculation, as applied to the general field of colloid chemistry (Feign and Napper, 1980; Jenkins and Vincent, 1996; Vincent, 1990; Vincent et al., 1986). However, polymer depletion as a mechanism for RBC aggregation has received much less attention with only a few literature reports relevant to this approach (Armstrong et al., 2001; Bäumler and Donath, 1987; Bäumler et al., 1996; Neu and Meiselman, 2001; Neu et al., 2002; van Oss et al., 1990). The present work was thus undertaken to develop a theoretical, quantitative understanding of the interactional energies involved in depletion-mediated RBC aggregation. The study was also designed to provide a qualitative description of polymer-induced RBC aggregation to examine the effects of polymer and RBC characteristics and thus to allow comparisons to previous literature data.

THEORY

To calculate surface affinities between RBC when suspended in polymer solutions, it is first necessary to define the nature of the cell-cell interaction. The exterior RBC surface, termed the glycocalyx, consists of a complex layer of proteins and glycoproteins and bears a net negative charge that is primarily due to ionized sialic acid groups (Seaman, 1975). In the theoretical model used herein, only depletion and electrostatic interactions are considered. As shown below, owing to the high electrostatic repulsion, cell-cell distances at which minimal interaction energy (i.e., maximal surface affinity) occurs are always greater than twice the thickness of the cell's glycocalyx. Thus, steric

Submitted April 30, 2002, and accepted for publication June 28, 2002.

Address reprint requests to Dr. Björn Neu, Department of Physiology and Biophysics, Keck School of Medicine, 1333 San Pablo Street, MMR 626, Los Angeles, CA 90033. Tel.: 323-442-1267; Fax: 323-442-1617; E-mail: neu@usc.edu.

0006-3495/02/11/2482/09 $2.00

interactions between glycocalyx on adjacent RBC can be neglected. Further, calculated total interaction energies are in the order of 1 to 10 $\mu J/m^2$, whereas for cell separations greater than twice the glycocalyx thickness, van der Waals interactions are in the range of 10^{-2} $\mu J/m^2$ (Lerche, 1984) and thus can also be neglected.

Depletion interaction

If a surface is in contact with a polymer solution and the loss of configurational entropy of the polymer is not balanced by adsorption energy, a depletion layer develops near the surface. Within this layer the polymer concentration is lower than in the bulk phase. Thus, as two RBC approach, the difference of solvent chemical potential (i.e., the osmotic pressure difference) between the intercellular polymer-poor depletion zone and the bulk phase results in solvent displacement into the bulk phase and hence depletion interaction. Due to this interaction, an attractive force develops that tends to minimize the polymer-reduced space between the cells (Fleer et al., 1993).

Depletion interaction energy

Examination of the energetics of depletion layers requires distinguishing between so-called "hard" and "soft or hairy" surfaces. Hard surfaces are considered to be smooth and do not allow polymer penetration into the surface, whereas soft surfaces, such as the RBC glycocalyx, are characterized by a layer of attached macromolecules that can be penetrated in part or entirely by the free polymer in solution (Jones and Vincent, 1989; Vincent et al., 1986). Fig. 1 *A* presents a stylized representation of polymer concentrations adjacent to a cell or particle with a soft surface. The subscripts 1, 2, and 3 indicate, respectively, the solvent, the free polymer in solution, and the polymer attached to the surface; δ indicates the thickness of the attached polymer layer, and p the penetration depth of the free polymer into the attached layer.

The depletion interaction energy w_D can be calculated by assuming a step profile for the free polymer as shown schematically in Fig. 1 *B* (Fleer et al., 1984; Vincent et al., 1986). Given a depletion layer thickness Δ and a separation distance of d between adjacent surfaces, w_D is given by

$$w_D = -2\Pi\left(\Delta - \frac{d}{2} + \delta - p\right) \qquad (1)$$

when $(d/2 - \delta + p) < \Delta$ and equals zero for $(d/2 - \delta + p) > \Delta$. The osmotic pressure term Π is calculated using a viral equation neglecting all coefficients higher than the second (B_2):

$$\Pi = \frac{RT}{M_2} c_2^b + B_2 (c_2^b)^2 = -\frac{(\mu_1 - \mu_1^0)}{v_1} \qquad (2)$$

in which R, T, v_1, and M_2 are the gas constant, absolute temperature, molecular volume of the solvent, and the molecular weight of the polymer. The chemical potential of the solvent in the polymer solution is μ_1 and is μ_1^0 in polymer free solution; c_2^b represents the bulk polymer concentration.

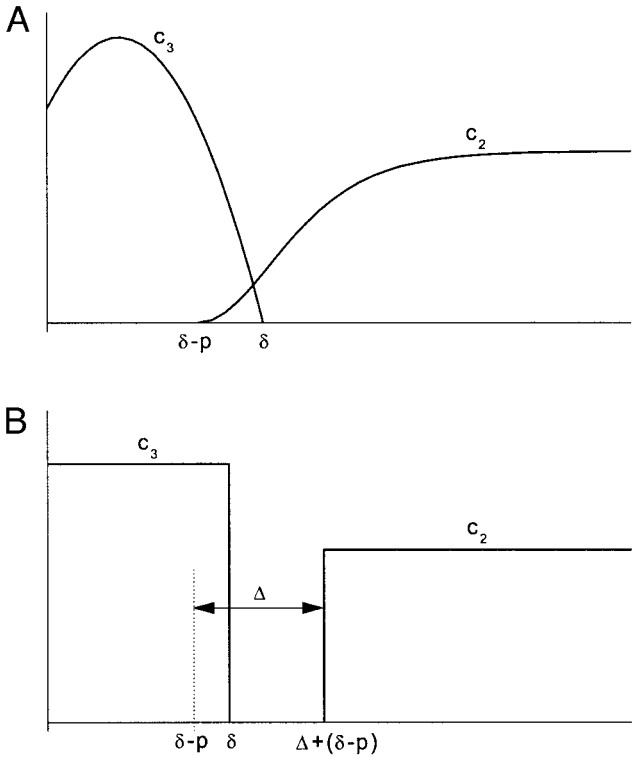

FIGURE 1 Concentration-distance profiles near a surface having an attached layer of polymer. Subscripts 1, 2, and 3 indicate solvent, free polymer, and attached polymer, respectively; δ, thickness of attached polymer layer; p, penetration depth of free polymer; Δ, depletion layer thickness. Fig. 1 *A* represents a stylized representation, whereas Fig. 1 *B* indicates the step profile used to calculate depletion interaction energy.

Depletion layer thickness

An approach introduced by Vincent (1990) is used to calculate the depletion layer thickness (Δ). This approach is based upon calculation of the equilibrium between the compressional or elastic free energy and the osmotic force experienced by polymer chains at a nonabsorbing surface and yields:

$$\Delta = -\frac{1}{2}\frac{\Pi}{D} + \frac{1}{2}\sqrt{\left(\frac{\Pi}{D}\right)^2 + 4\Delta_0^2} \qquad (3)$$

in which Π is the osmotic pressure of the bulk polymer solution. The parameter D is a function of the bulk polymer concentration (c_2^b):

$$D = \frac{2k_B T}{\Delta_0^2}\left(\frac{c_2^b N_a}{M_2}\right)^{2/3} \qquad (4)$$

in which k_B and N_a are the Boltzmann constant and Avogadro number. Δ_0 is the depletion thickness for vanishing

polymer concentration and is equal to $1.4 \times R_g$, in which R_g is the polymer's radius of gyration (Vincent, 1990).

Penetration depth

Intuitively, the penetration depth p of the free polymer into the attached layer should depend on the polymer type, concentration, and molecular size, and would be expected to be larger for small molecules and to increase with increasing polymer concentration due to increasing osmotic pressure. One possibility is to calculate p by assuming that penetration proceeds until the local osmotic pressure developed in the attached layer is balanced by the osmotic pressure of the bulk solution (Vincent et al., 1986). It is also possible to consider that the attached polymers collapse under the osmotic pressure of the bulk polymer (Jones and Vincent, 1989). However, it is difficult to accurately apply such a model to RBC in polymer or protein solutions since too little is known about the physicochemical properties of the glycocalyx, and in particular, about the interaction between the glycocalyx and different polymers or proteins. Thus, an exponential approximation for the concentration dependence of the penetration depth is used:

$$p = \delta\left(1 - e^{-c_2^b/c_2^p}\right) \tag{5}$$

in which c_2^p is the penetration constant of the polymer in solution (i.e., when c_2^p equals c_2^b, p is 63% of δ). In this approach δ is assumed to be independent of bulk polymer concentration. Therefore p is essentially a linear function of c_2^b at low concentrations (relative to c_2^p) and asymptotically approaches δ at high concentrations.

Electrostatic interaction

The electrostatic free energy of two cells can be calculated by simply considering an isothermal charging process:

$$E = \frac{1}{2}\int_0^d \int_0^\rho \psi(\rho, x) d\rho dx \tag{6}$$

in which ψ is the electrostatic potential between the cells, which is dependent on the charge density ρ. To calculate the electrostatic interaction energy between two cells, one first calculates the free energy of the two cells at a separation distance d, and then deducts the free energy of two single cells (i.e., as $d \to \infty$).

To calculate the electrostatic potential ψ for RBC, it is necessary to solve the Poisson-Boltzmann equation; the linear approximation that is usually suitable for moderate electric potentials is used herein (Bäumler et al., 1996). Assuming that both cells have the same constant charge and that it is evenly distributed within the glycocalyx (i.e., same profile as c_3 in Fig. 1), ψ can be calculated for a single cell surface and for two cells at a separation distance d. However, it is possible to simplify this approach by approximating the electrostatic potential between two cells as a superposition of the potential of two single cells. This simplification is possible since the Debye-Hückel length is small compared with both the glycocalyx thickness δ and the calculated cell-cell distance d. For the parameters used herein (see below) the difference due to this simplification is less than 0.1% for $d \geq 2 \times \delta$. Using this superposition the electrostatic interaction energy w_E is:

$$w_E = \frac{\sigma^2}{\delta^2 \varepsilon \varepsilon_0 \kappa^3} \begin{cases} \sinh(\kappa\delta)(e^{\kappa\delta - \kappa d} - e^{-\kappa d}) & d \geq 2\delta \\ (2\kappa\delta - \kappa d) - (e^{-\kappa\delta} + 1)\sinh(\kappa\delta - \kappa d) - \sinh(\kappa\delta)e^{-\kappa d} & d < 2\delta \end{cases} \tag{7}$$

in which ϵ and ϵ_o are the relative permittivity of the solvent and the permittivity of vacuum.

Finally, the total interaction energy w_T per unit area of cell surface is given by the sum of Eqs. 1 and 7:

$$w_T = w_D + w_E \tag{8}$$

RESULTS

Polymer and RBC parameters

To provide calculated results relevant to published data for polymer-induced RBC aggregation (Boynard and Leliere, 1990; Brooks, 1988; Chien et al., 1987; Nash et al., 1987), emphasis was directed toward two types of flexible, nonionic, water soluble polymers: 1) dextran, abbreviated as DEX, which is a long chain of glucose units joined primarily by 1:6 α links with some 1:3 and 1:4 links; 2) poly (ethylene glycol), abbreviated as PEG, which is a repeating linear chain of ethylene oxide. Both polymers are available in several molecular weight fractions, and their physicochemical properties have been studied in detail. Table 1 presents osmotic viral coefficients (B_2) and molecular size as radius of gyration (R_g) for the DEX and PEG polymers considered herein. The RBC glycocalyx thickness δ was held constant at 5 nm and a value of 0.036 C/m^2 was

TABLE 1 Physicochemical properties of polymers

	Dextran					Poly (ethylene glycol)	
MW_w (kDa)	40	70	150	250	500	18	35
B_2 ($m^5s^{-2}kg^{-1}$)	2.50	1.69	0.99	0.69	0.43	6.93	6.40
R_g (nm)	5.57	7.36	10.8	13.9	19.7	4.60	6.42

MW_w, Weight average molecular mass; B_2, second viral coefficient; R_g, radius of gyration.

Values (at 25°C) estimated from literature data (Hasse et al., 1995; Haynes et al., 1989; Ioan et al., 2001; Kany et al., 1999; Krabi and Donath, 1994; Nordmeier, 1993; Nordmeier et al., 1993; Smit et al., 1992).

R_g calculated as $R_g = A_{ec}M_w^{0.5}$ with A_{ec}(DEX) = 0.88 nm × $mol^{0.5}$ × $kg^{-0.5}$ and A_{ec}(PEG) = 1.09 nm × $mol^{0.5}$ × $kg^{-0.5}$.

assumed for the RBC surface charge density σ (Donath et al., 1996; Donath and Voigt, 1985; Levine et al., 1983), and a value of 0.76 nm was used as the Debye-Hückel length κ^{-1} (Bäumler et al., 1996).

Depletion layer thickness and interaction energy

Fig. 2 presents depletion layer thickness (Δ) values, calculated via Eq. 3, as a function of bulk polymer concentration (c_2^b) for 70-, 150-, and 500-kDa dextran and for 35-kDa PEG. These results indicate: 1) at lower c_2^b levels (i.e., <1 g/dL), Δ decreases only slightly with increasing concentration, whereas at higher concentrations the depletion layer thickness decreases rapidly; 2) for a specific polymer type (e.g., dextran), depletion layer thickness increases with increasing molecular mass and hence with increasing size (i.e., see R_g, Table 1); 3) polymer physicochemical properties other than molecular mass can affect depletion layer thickness (e.g., nearly comparable Δ values for PEG 35 and DEX 70).

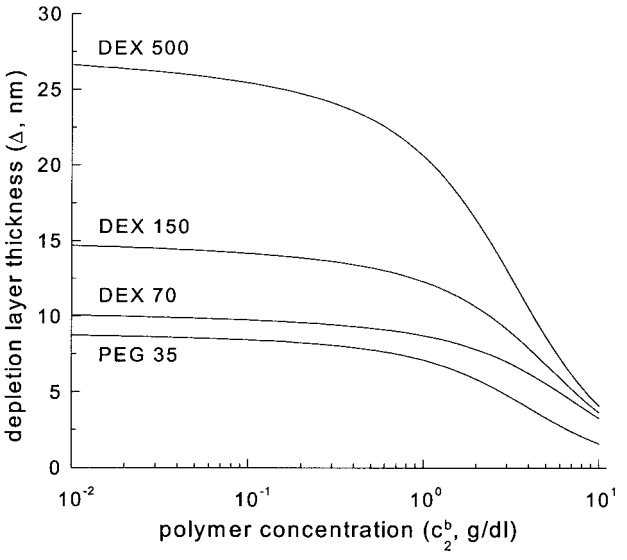

FIGURE 2 Effects of bulk phase polymer concentration ($c^b{}_2$) on depletion layer thickness (Δ) for 70, 150, and 500 kDa dextrans and 35 kDa poly(ethylene glycol).

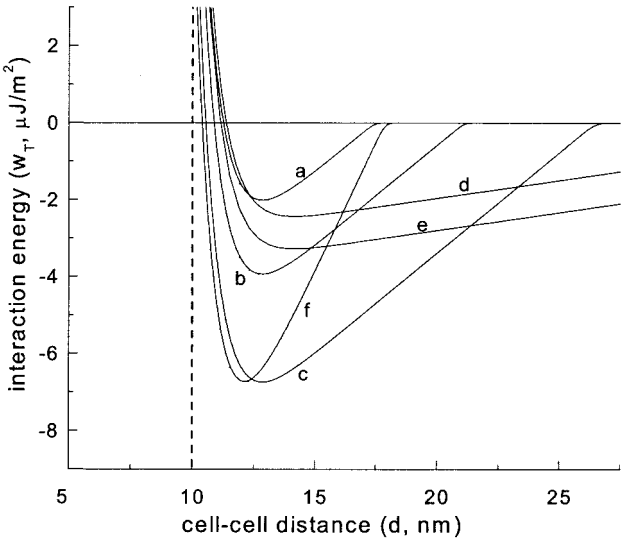

FIGURE 3 Effects of penetration constant (c_2^p) on total interactional energy (w_T) versus RBC-RBC separation (d) for cells in DEX 70 ((*a*) $c_2^p \rightarrow 0$, (*b*) c_2^p = 1 g/dL, (*c*) c_2^p = 10 g/dL), DEX 500 ((*d*) $c_2^p \rightarrow 0$, (*e*) c_2^p = 1 g/dL), and PEG 35 ((*f*) c_2^p = 1 g/dL) with a constant polymer concentration (c_2^b) of 1 g/dL. The dashed vertical line at 10 nm indicates the total glycocalyx thickness for both cells (i.e., 5 nm per cell).

The effects of cell-cell separation distance (d) on total surface interaction energy (w_T) are shown in Fig. 3 for DEX 70, DEX 500, and PEG 35. In this figure, the bulk polymer concentration c_2^b was held constant at 1 g/dL, and various values of the penetration constant c_2^p were used. The calculated results shown clearly demonstrate the impact of the penetration constant as well as of polymer type and size (i.e., molecular mass). For example, DEX 70 has a more pronounced dependence on the penetration constant than DEX 500. For a change of c_2^p from 0 to 10 g/dL, there is more than a threefold increase in interaction energy for DEX 70, whereas DEX 500 shows only approximately a 30% increase. This unequal dependency on the penetration constant seems consistent with polymer size versus glycocalyx thickness. Because the R_g of DEX 500 is approximately four times greater than the 5-nm-thick RBC glycocalyx (Table 1), the impact of the penetration constant on the interaction energy is rather small. Conversely, the R_g for DEX 70 is only ~50% larger than the glycocalyx thickness, and thus glycocalyx penetration can markedly affect w_T.

Also shown in Fig. 3 is the interaction energy (w_T) for PEG 35 with a penetration constant c_2^p of 1 g/dL (curve f). Clearly PEG 35 exhibits a higher maximal value of w_T than DEX 70 for c_2^p equal to unity (curve b). This difference of maximal w_T for PEG 35 and DEX 70 is due to their different physicochemical properties. Although these molecules have about the same R_g (Table 1) and thus about the same Δ for c_2^b = 1 g/dL (Fig. 2), the molar concentration of PEG 35 is

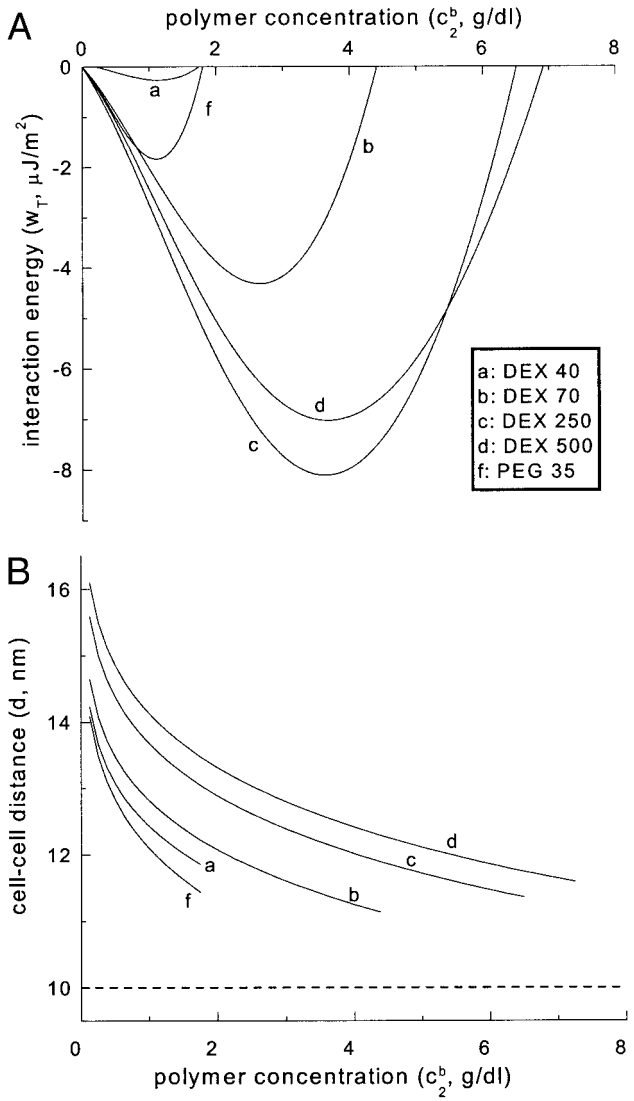

FIGURE 4 Effects of bulk phase polymer concentration (c_2^b) on total interactional energy w_T (Fig. 4 *A*) and cell-cell separation *d* (Fig. 4 *B*) for RBC suspended in various molecular mass fractions of dextran and poly-(ethylene glycol). The penetration *p* was set equal to δ (i.e., maximal penetration depth independent of c_2^b). Because with *p* set to δ the interactional energy for PEG 18 is zero, lines for this polymer are not shown.

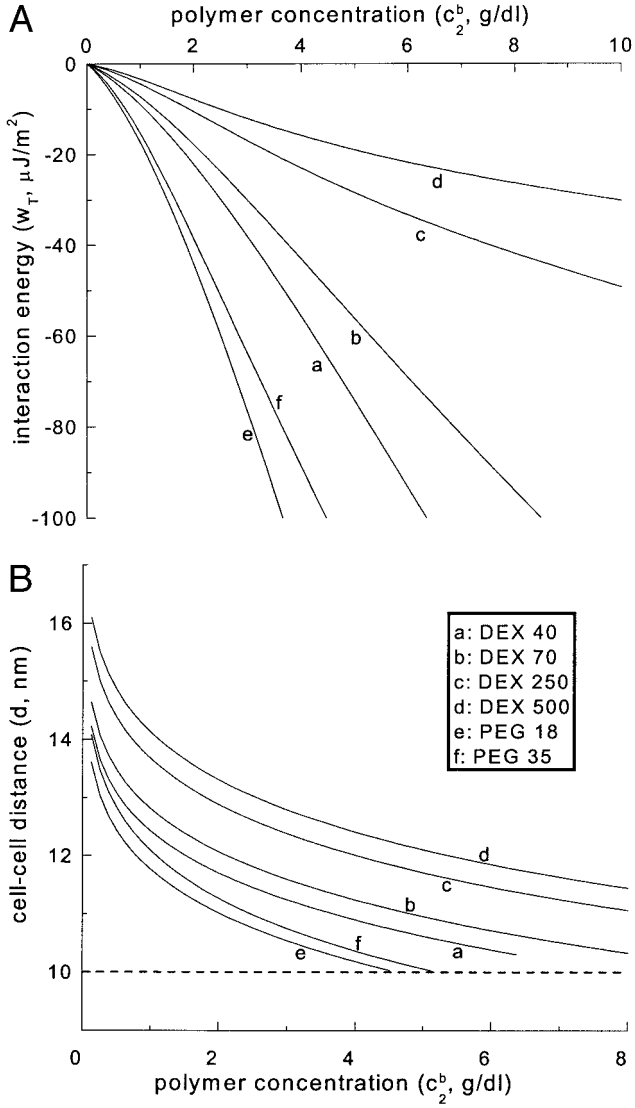

FIGURE 5 Effects of bulk phase polymer concentration (c_2^b) on total interactional energy w_T (Fig. 5 *A*) and cell-cell separation *d* (Fig. 5 *B*) for RBC suspended in various molecular mass fractions of dextran and poly-(ethylene glycol). The penetration *p* was set equal to 0 (i.e., no penetration regardless of c_2^b).

twofold greater than DEX 70. This difference of molar concentration leads to approximately twice the osmotic pressure difference between the depletion layer and the bulk phase (Eq. 2), and therefore the doubled interactional energy for PEG 35 is expected.

The effects of bulk phase polymer concentration (c_2^b) on maximal interaction energy are shown in Figs. 4 *A* and 5 *A* with the corresponding cell-cell separation distances shown in Figs. 4 *B* and 5 *B*. The maximal interaction energies represent the nadir of the w_T versus separation distance for each polymer. In Fig. 4 the penetration *p* was set to δ (i.e., $c_2^p \rightarrow 0$), indicating maximal penetration depth independent of polymer concentration, whereas in Fig. 5 *p* was set equal to 0 (i.e., $c_2^p \rightarrow \infty$), indicating no penetration of the free polymers into the glycocalyx regardless of bulk phase polymer concentration.

Within the plotted concentration range, penetration of polymer into the glycocalyx (Fig. 4 *A*) results in $w_T - c_2^b$ relations that are bell shaped and concave to the concentration axis, and for a given polymer type show increasing maximal values of w_T with increasing molecular mass. In contrast, a lack of penetration into the glycocalyx (Fig. 5 *A*) yields essentially linear $w_T - c_2^b$ relations and markedly higher levels of w_T; smaller molecules result in higher

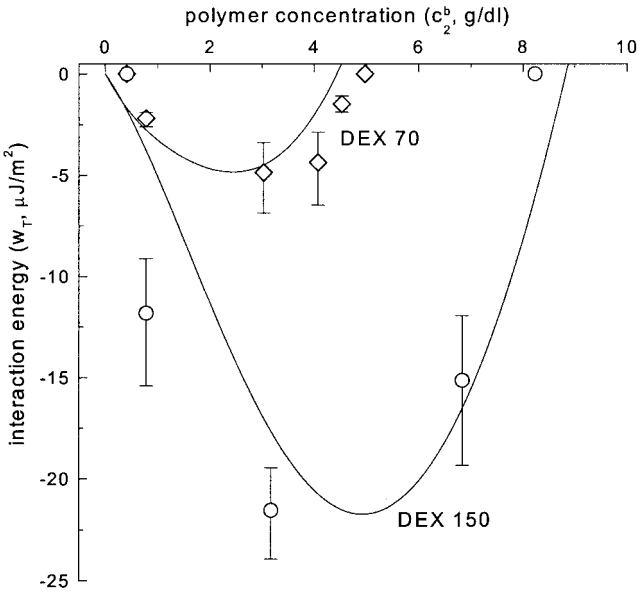

FIGURE 6 Comparisons between calculated (*solid lines*) and experimental (data points from Buxbaum et al., 1982) values of interactional energy (w_T) for RBC suspended in various concentrations of DEX 70 or DEX 150.

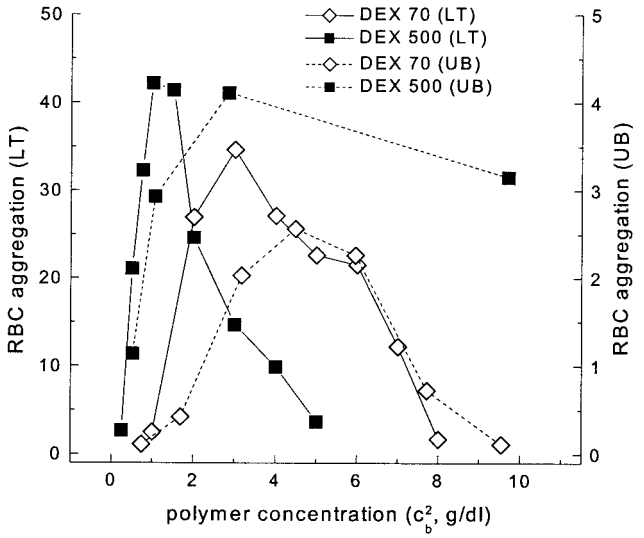

FIGURE 7 Polymer concentration-RBC aggregation results for cells suspended in solutions of DEX 70 or DEX 500. Light transmission data (LT) from Nash et al. (1987) and ultrasound backscatter data (UB) from Boynard and Leliere (1990).

values, because the effect of the greater osmotic pressure difference outweighs the influence of the larger depletion layer for the bigger molecules. The calculated cell-cell separation distances are much less sensitive to the magnitude of the penetration constant (Figs. 4 *B* and 5 *B*). These distances decrease with increasing bulk phase polymer concentration, and for the same polymer type, increase with increasing polymer molecular mass.

DISCUSSION

Using micropipette techniques to measure the extent of encapsulation of an RBC membrane sphere by an intact RBC, Buxbaum et al. (1982) determined cell-cell surface affinities for normal human red blood cells in various dextran solutions. Their results, based on a scheme wherein the extent of encapsulation reflects surface affinity versus membrane shear elastic modulus, indicate biphasic affinity-concentration relations with peak surface affinities of 4.9 μJ/m^2 for 70 kDa dextran and 22 μJ/m^2 for 150 kDa dextran (Fig. 6).

To quantitatively compare these experimental findings with interactional energies calculated via the present model, the penetration constant c_2^p was varied until the calculated peak interactional energy for DEX 70 or DEX 150 equaled the value reported by Buxbaum et al. (i.e., c_2^p was the only parameter varied). This equality with their peak data occurred at $c_2^p = 0.70$ g/dL for DEX 70 and $c_2^p = 7.5$ g/dL for DEX 150; calculated $w_T - c_2^b$ relations based upon these c_2^p values are shown as solid lines in Fig. 6. The shapes of the calculated $w_T - c_2^b$ relations and the upper polymer concentrations at which w_T declines to zero are in excellent agreement with their experimental data. In addition, the values of c_2^p required to achieve equality between the calculated and experimental peak w_T levels are consistent with the expected effect of polymer molecular mass on glycocalyx penetration (i.e., lower value of c_2^p for DEX 70 indicating greater penetration ability for smaller dextran molecules).

RBC aggregation has been studied using a variety of testing systems (e.g., light reflection or transmission, microscopy, ultrasound, viscometry), and numerous investigators have described the effects of polymer concentration and molecular mass on RBC aggregation (Boynard and Leliere, 1990; Brooks, 1988; Chien et al., 1987; Nash et al., 1987). Representative aggregation data, obtained via light transmission and ultrasound backscattering methods for RBC suspended in isotonic solutions of DEX 70 and DEX 500 are shown in Fig. 7. These experimental data reflect two typical aspects of polymer-induced RBC aggregation: 1) biphasic, bell-shaped response to polymer concentration and 2) for a given polymer type (e.g., dextran), the extent or strength of aggregation increases with molecular mass. Owing to the empirical indices used to determine RBC aggregation, quantitative comparisons to calculated cell-cell affinities are precluded. However, the experimental findings shown in Fig. 7 are in qualitative agreement with the shape and position of the calculated w_T results presented in Figs. 4 *A* and 6.

The computed results for w_T, combined with experimental findings for RBC aggregation (e.g., Fig. 7), clearly indicate that changes of interactional energy are mirrored by

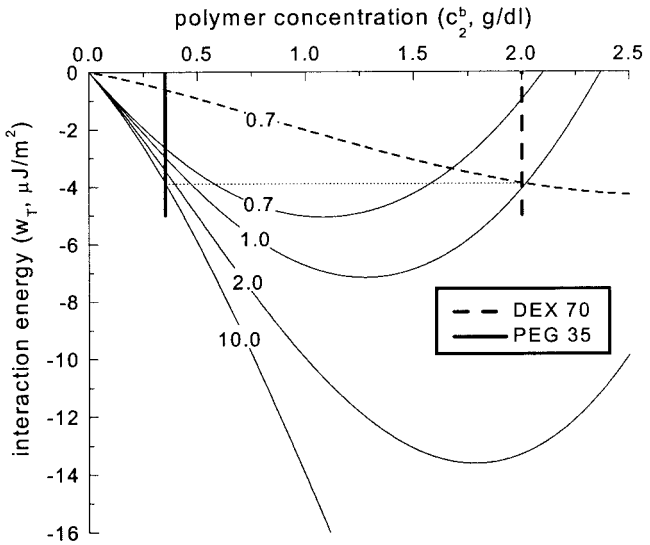

FIGURE 8 Graphical approach to estimating penetration constant c_2^p for PEG 35. Vertical lines indicate polymer concentrations for equal RBC aggregation in PEG 35 (0.35 g/dL) and in DEX 70 (2 g/dL); curved lines indicate $c_2^p = 0.7$ g/dL for DEX 70 (Fig. 6) and various c_2^p values for PEG 35 (in g/dL).

changes of RBC aggregation. Increased interactional energy increases RBC aggregation, whereas reduced interactional energy reduces aggregation. However, the relative importance of factors causing changes of w_T does differ between the ascending and descending regions of the aggregation-concentration relation. In the ascending region, w_T increases since the depletion layer thickness (Δ, Fig. 2) and thus the bracketed terms in Eq. 1 remain relatively constant (Fig. 2), whereas the osmotic pressure difference increases (Eq. 2). In the descending region, w_T decreases since the effects of the markedly reduced depletion layer thickness (Fig. 2, Eq. 1) outweigh the effects of the increased osmotic pressure difference.

The model deployed herein allows insight into polymer-glycocalyx interactions obtained with different types of macromolecules. For example, at comparable polymer molecular mass and polymer concentration, RBC aggregation is usually much stronger in PEG than in dextran solutions (Neu et al., 2001): despite a nearly sixfold difference in concentration, equal RBC aggregation occurs for cells in 0.35 g/dL PEG 35 and in 2 g/dL DEX 70. Fig. 8 presents calculated interactional energy-concentration relations for DEX 70 at $c_2^p = 0.7$ g/dL and for PEG 35 at several values of c_2^p. Also shown in Fig. 8 are vertical lines at the PEG 35 and DEX 70 concentrations yielding equal RBC aggregation, and a dashed horizontal line originating at the intersection of the DEX 70 curve ($c_2^p = 0.7$ g/dL) and the DEX 70 vertical line. The horizontal dashed line intersects the PEG 35 vertical line at a c_2^p value of ~10 g/dL. Thus, even though PEG 35 and DEX 70 have approximately the same radius of gyration (Table 1), the value of c_2^p for PEG 35 is multifold higher than the value of 0.7 g/dL for DEX 70. The higher value of c_2^p for PEG 35 indicates less penetration of the glycocalyx and therefore a lower affinity of PEG 35 for the constituents of the RBC glycocalyx.

Although the current model appears robust, there are areas that require further attention. For example, a strong effect of dextran molecular mass on intercellular separation for aggregated RBC (e.g., 18 nm for DEX 40 and 30 nm for DEX 500) has been previously reported (Chien and Jan, 1973), whereas over the same molecular mass range our calculated separations increase by only ~15% (Figs. 4 *B* and 5 *B*). However, it should be noted that our separations were calculated for maximal interactional energies, and that for large dextrans the w_T-separation relations are fairly shallow (Fig. 3, curves d and e). Thus, for these larger polymers, cell-cell separation might be greater without a major decrease of interactional energy.

Further, the present model does not consider polymer adsorption onto the RBC surface and hence the possible effects of steric interactions or altered depletion layer thickness due to adsorbed polymer (van Oss et al., 1990). Bäumler et al. (2001) suggest an inverse association between polymer adsorption and RBC aggregation, and experimental results for dextran adsorption onto human RBC have been presented (Brooks et al., 1980; Chien et al., 1977). However, Janzen and Brooks (1991) indicate that RBC adsorption data for dextran and proteins are subject to numerous potential artifacts and are quantitatively difficult to interpret, thus making tenuous their application to the current model. The effects of abnormal RBC rheological behavior have also not been considered (Evans, 1989), although they are acknowledged to potentially affect relations between calculated w_T and measured RBC aggregation. Red blood cells rigidified by heat treatment or chemical fixation are known to exhibit markedly decreased aggregation (Nash et al., 1987).

In overview, our results indicate that an approach that considers polymer depletion and electrostatic repulsion is in qualitative and quantitative agreement with experimental measures of cell-cell affinity and RBC aggregation. It is acknowledged that it represents a somewhat simplified approach, and thus requires additional theoretical and experimental focus on more realistic treatments of the RBC glycocalyx and on interactions between the glycocalyx and charged or neutral polymers or proteins. Charge distribution within the glycocalyx also needs to be considered since it has a significant effect on electrostatic interactional energy (Lerche, 1984). Further, it would be of interest to apply this model to presently unresolved aspects of human RBC aggregation, such as the more than 100% increase of aggregation for old versus young RBC when suspended in autologous plasma or polymer solutions (Meiselman, 1993), or the reduced aggregation of neonatal red cells in plasma or in polymer solutions (Linderkamp et al., 1984). Application of this model may also be of potential value in human disease.

Disturbed in vivo blood flow consequent to elevated RBC aggregation has been observed in clinical states such as diabetes mellitus, myocardial infarction, and renal disease (Lowe, 1988), and a clearer understanding of polymer-glycocalyx interactions should allow rationale development of therapeutic agents.

Supported by Deutsche Forschungsgemeinschaft Grant NE 784/1-2 (to B.N.) and the National Institutes of Health Research Grants HL15722 and HL48484 (to H.J.M.).

REFERENCES

Armstrong, J. K., H. J. Meiselman, R. B. Wenby, and T. C. Fisher. 2001. Modulation of red blood cell aggregation and blood viscosity by the covalent attachment of Pluronic copolymers. *Biorheology.* 38:239–247.

Bäumler, H., and E. Donath. 1987. Does dextran indeed significantly increase the surface potential of human red blood cells? *Stud. Biophys.* 120:113–122.

Bäumler, H., E. Donath, A. Krabi, W. Knippel, A. Budde, and H. Kiesewetter. 1996. Electrophoresis of human red blood cells and platelets: evidence for depletion of dextran. *Biorheology.* 33:333–351.

Bäumler, H., B. Neu, R. Mitlohner, R. Georgieva, H. J. Meiselman, and H. Kiesewetter. 2001. Electrophoretic and aggregation behavior of bovine, horse and human red blood cells in plasma and in polymer solutions. *Biorheology.* 38:39–51.

Boynard, M., and J. C. Leliere. 1990. Size determination of red blood cell aggregates induced by dextran using ultrasound backscattering phenomenon. *Biorheology.* 27:39–46.

Brooks, D. E. 1973. The effect of neutral polymers on the electrokinetic potential of cells and other charged particles. *J. Colloid Interface Sci.* 43:700–713.

Brooks, D. E. 1988. Mechanism of red cell aggregation. *In* Blood Cells, Rheology and Aging. D. Platt, editor. Springer Verlag, Berlin. 158–162.

Brooks, D. E., R. G. Greig, and J. Janzen. 1980. Mechanism of erythrocyte aggregation. *In* Erythrocyte Mechanics and Blood Flow. G. R. Cokelet, H. J. Meiselman, D. E. Brooks, editors. A.R. Liss, New York. 119–140.

Buxbaum, K., E. Evans, and D. E. Brooks. 1982. Quantitation of surface affinities of red blood cells in dextran solutions and plasma. *Biochemistry.* 21:3235–3239.

Cabel, M., H. J. Meiselman, A. S. Popel, and P. C. Johnson. 1997. Contribution of red blood cell aggregation to venous vascular resistance in skeletal muscle. *Am. J. Physiol. Heart Circul. Physiol.* 41: H1020–H1032.

Chien, S. 1975. Biophysical behavior of red cells in suspensions. *In* The Red Blood Cell. D.M. Surgenor, editor. Academic Press, New York. 1031–1133.

Chien, S., J. Dormandy, E. Ernst, and A. Matrai. 1987. Clinical Hemorheology. M. Nijhoff Publishers, Boston, MA.

Chien, S., and K. M. Jan. 1973. Ultrastructural basis of the mechanism of rouleaux formation. *Microvasc. Res.* 5:155–166.

Chien, S., and L. A. Lang. 1987. Physicochemical basis and clinical implications of red cell aggregation. *Clin. Hemorheol.* 7:71–91.

Chien, S., S. Simchon, R. E. Abbot, and K. M. Jan. 1977. Surface adsorption of dextrans on human red cell membrane. *J. Colloid Interface Sci.* 62:461–470.

Cloutier, G., and Z. Qin. 1997. Ultrasound backscattering from non-aggregating and aggregating erythrocytes: a review. *Biorheology.* 34: 443–470.

Donath, E., A. Budde, E. Knippel, and H. Baumler. 1996. "Hairy surface layer" concept of electrophoresis combined with local fixed surface charge density isotherms: application to human erythrocyte electrophoretic fingerprinting. *Langmuir.* 12:4832–4839.

Donath, E., and A. Voigt. 1985. Influence of surface structure on cell electrophoresis. *In* Cell Electrophoresis. W. Schütt and H. Klinkmann, editors. De Gruyter, Berlin, New York. 123–135.

Evans, E., and K. Buxbaum. 1981. Affinity of red blood cell membrane for particle surfaces measured by the extent of particle encapsulation. *Biophys. J.* 34:1–12.

Evans, E. A. 1989. Structure and deformation properties of red blood cells: concepts and quantitative methods. *Methods Enzymol.* 173:3–35.

Evans, E. A., and V. A. Parsegian. 1983. Energetics of membrane deformation and adhesion in cell and vesicle aggregation. *Ann. N. Y. Acad. Sci.* 416:13–33.

Feign, R. I., and D. H. Napper. 1980. Depletion stabilization and depletion flocculation. *J. Colloid Interface Sci.* 75:525–541.

Fleer, G. J., M. A. Cohen Stuart, J. H. M. H. Scheutjens, T. Cosgrove, and B. Vincent. 1993. Polymers at interfaces. Chapman and Hall, London.

Fleer, G. J., J. H. M. H. Scheutjens, and B. Vincent. 1984. The stability of dispersions of hard spherical particles in the presence of nonadsorbing polymer. *In* Polymer adsorption and dispersion stability. E. D. Goddard and B. Vincent, editors. ACS, Washington, DC. 245–263.

Hasse, H., H. P. Kany, R. Tintinger, and G. Maurer. 1995. Osmotic virial-coefficients of aqueous poly(ethylene glycol) from laser-light scattering and isopiestic measurements. *Macromolecules.* 28:3540–3552.

Haynes, C. A., R. A. Beynon, R. S. King, H. W. Blanch, and J. M. Prausnitz. 1989. Thermodynamic properties of aqueous polymer-solutions - poly(ethylene glycol) dextran. *J. Phys. Chem.* 93:5612–5617.

Holley, L., N. Woodland, W. T. Hung, K. Cordatos, and A. Reuben. 1999. Influence of fibrinogen and haematocrit on erythrocyte sedimentation kinetics. *Biorheology.* 36:287–297.

Hovav, T., S. Yedgar, N. Manny, and G. Barshtein. 1999. Alteration of red cell aggregability and shape during blood storage. *Transfusion.* 39: 277–281.

Ioan, C. E., T. Aberle, and W. Burchard. 2001. Light scattering and viscosity behavior of dextran in semidilute solution. *Macromolecules.* 34:326–336.

Janzen, J., and D. E. Brooks. 1991. A critical reevaluation of the nonspecific adsorption of plasma proteins and dextrans to erythrocytes and the role of these in rouleaux formation. *In* Interfacial Phenomena in Biological Systems. M. Bender, editor. Marcel Dekker, New York. 193–250.

Jenkins, P., and B. Vincent. 1996. Depletion flocculation of nonaqueous dispersions containing binary mixtures of nonadsorbing polymers: evidence for nonequilibrium effects. *Langmuir.* 12:3107–3113.

Jones, A., and B. Vincent. 1989. Depletion flocculation in dispersions of sterically-stabilized particles 2: modifications to theory and further-studies. *Colloids Surfaces* 42:113–138.

Kany, H. P., H. Hasse, and G. Maurer. 1999. Thermodynamic properties of aqueous dextran solutions from laser-light-scattering, membrane osmometry, and isopiestic measurements. *J. Chem. Eng. Data.* 44: 230–242.

Kounov, N. B., and V. G. Petrov. 1999. Determination of erythrocyte aggregation. *Math. Biosci.* 157:345–356.

Krabi, A., and E. Donath. 1994. Polymer depletion layers as measured by electrophoresis. *Colloid Surf. A. Physicochem. Eng. Asp.* 92:175–182.

Lerche, D. 1984. Electrostatic fixed charge distribution in the RBC-glycocalyx and their influence upon the total free interaction energy. *Biorheology.* 21:477–492.

Levine, S., M. Levine, K. A. Sharp, and D. E. Brooks. 1983. Theory of the electrokinetic behavior of human erythrocytes. *Biophys. J.* 42:127–135.

Lim, B., P. A. J. Bascom, and R. S. C. Cobbold. 1997. Simulation of red blood cell aggregation in smear flow. *Biorheology* 34:423–441.

Linderkamp, O., P. Ozanne, P. Y. Wu, and H. J. Meiselman. 1984. Red blood cell aggregation in preterm and term neonates and adults. *Pediatr. Res.* 18:1356–1360.

Lowe, G. D. O. 1988. Clinical Blood Rheology. CRC Press, Boca Raton, FL.

Meiselman, H. J. 1993. Red-blood-cell role in RBC aggregation. *Clin. Hemorheol.* 13:575–592.

Meiselman, H. J., O. K. Baskurt, S. O. Sowemimo-Coker, and R. B. Wenby. 1999. Cell electrophoresis studies relevant to red blood cell aggregation. *Biorheology.* 36:427–432.

Nash, G. B., R. B. Wenby, S. O. Sowemimo-Coker, and H. J. Meiselman. 1987. Influence of cellular properties on red cell aggregation. *Clin. Hemorheol.* 7:93–108.

Neu, B., J. K. Armstrong, T. C. Fisher, and H. J. Meiselman. 2001. Aggregation of human RBC in binary dextran-PEG polymer mixtures. *Biorheology* 38:53–68.

Neu, B., and H. J. Meiselman. 2001. Sedimentation and electrophoretic mobility behavior of human red blood cells in various dextran solutions. *Langmuir.* 17:7973–7975.

Neu, B., H. J. Meiselman, and H. Bäumler. 2002. Electrophoretic mobility of human erythrocytes in the presence of poly (styrene sulfonate). *Electrophoresis* 23:2363–2368.

Nordmeier, E. 1993. Static and dynamic light-scattering solution behavior of pullulan and dextran in comparison. *J. Phys. Chem.* 97:5770–5785.

Nordmeier, E., H. Xing, and M. D. Lechner. 1993. Static and dynamic light-scattering-studies of dextran from leuconostoc-mesenteroides in the dilute region. *Makromol. Chem.* 194:2923–2937.

Seaman, G. V. F. 1975. Electrokinetic behavior of red cells. *In* The Red Blood Cell. D. M. Surgenor, editor. Academic Press, New York. 1135–1229.

Sennaoui, A., M. Boynard, and C. Pautou. 1997. Characterization of red blood cell aggregate formation using an analytical model of the ultrasonic backscattering coefficient. *IEEE Trans. Biomed. Eng.* 44:585–591.

Smit, J. A. M., J. Vandijk, M. G. Mennen, and M. Daoud. 1992. Polymer size exponents of branched dextrans. *Macromolecules.* 25:3585–3590.

Stoltz, J. F., M. Singh, and P. Riha. 1999. Hemorheology in Practice. IOS Press, Amsterdam.

van Oss, C. J., K. Arnold, and W. T. Coakley. 1990. Depletion flocculation and depletion stabilization of erythrocytes. *Cell Biophys.* 17:1–10.

Vincent, B. 1990. The calculation of depletion layer thickness as a function of bulk polymer concentration. *Colloids Surfaces.* 50:241–249.

Vincent, B., J. Edwards, S. Emmett, and A. Jones. 1986. Depletion flocculation in dispersions of sterically-stabilised particles (“soft spheres”). *Colloids Surfaces.* 18:261–281.